İstanbul Yerbilimleri Dergisi, C.26, S.1, SS. 25-35, Y. 2013

LINEAMENT DETECTION FROM GRAVITY ANOMALY MAPS WITH THE GRADIENT HOUGH ALGORITHM IN ADAPAZARI BASIN

ADAPAZARI HAVZASINDA GRADİYENT HOUGH ALGORİTMASI İLE GRAVİTE ANOMALİ HARİTALARINDAN ÇİZGİSELLİK SAPTAMA

Davut Aydogan[1] and Masao Komazawa[2]

[1] Istanbul Üniversitesi, Mühendislik Fakültesi, Jeofizik Bölümü, 34320, Avcılar, Istanbul

[2] OYO Coporation, 43 Miyukigaoka, Tsukuba, Ibaraki 305-0841, Japan

ABSTRACT

As indicators of certain significant geological structural elements, linear anomalies are important in interpreting gravity and magnetic anomalies. Lineaments are usually mapped by using improved data. Numerous algorithms have been developed to automatize this process. This paper presents an integrated study of the Adapazari basin by taking into consideration a set of gravity data and surface geology. Subsurface geological modeling is performed by Hough transform (HT) based on gradient calculations as an image enhancement technique and an interpretation of the gravity values including boundary analysis algorithms. Application of the gravity method to structural geology helps shedding light on the local changes in the gravity gradient zones caused by density differences pertaining to crustal structure and composition. Anomalies occurring in gradient zones are commonly expressed as potential-field lineaments. The methods proposed to detect these discontinuities and boundaries corresponding to differences are tested on synthetic data as the initial stage and the results obtained are satisfactory. As the second stage, they are applied to the gravity anomaly map of the Adapazari basin and possible lineaments are automatically obtained. In addition to provide supportive data, sediment thickness in the region is computed by using 3DINVER matlab program. Automatic analysis results are compared to the major and minor faults depicted in the geological map of the study area. The results demonstrate that automatic lineament detection depicts more fault traces than visual interpretation. By combining the lineaments obtained with geological and supportive data, we try to introduce a new approach to tectonic development for the study area.

These examples demonstrate that in detecting the geological features defined as major and minor faults, the Hough algorithm can be used for qualitative interpretation of gravity anomaly maps.

Key words: Hough transform, boundary analysis, gravity, lineaments, Adapazari basin,Turkey.

ÖZ

Doğrusal anomaliler, bazı önemli jeolojik yapısal unsurların göstergeci olduklarından gravite ve manyetik anomalilerin yorumlanmasında önemlidir. Çizgisellikleri haritalama genelde iyileştirilmiş veriler kullanılarak yapılmaktadır. Bu işlemi otomatik hale getirmek için pek çok algoritma geliştirilmiştir. Bu çalışmada, gravite verileri ile yüzey jeolojisinin bir seti göz önünde tutularak Adapazari basenine ait tümleşik bir araştırma ortaya konmuştur. Yeryüzü altının jeolojik modelllenmesi, görüntü iyileştirme tekniklerinden olan gradiyent hesaplamalarına dayandırılmış Hough donüşümü (HT), ve sınır analizi algoritmalarını içeren gravite değerlerinin yorumu ile gerçekleştirilmiştir. Gravite yönteminin yapısal jeolojiye uygulanması, kabuk yapısı ve bileşimi ile ilgili olan yoğunluk farklılıklarının sebep olduğu gravite gradiyent zonlarının yerel değişimlerinin aydınlatılmasına imkan sağlar. Gradiyent zonlarında oluşan anomaliler genelde potansiyel alan çizgisellikleri olarak ifade edilirler. Farklılıklara karşılık gelen bu süreksizlikler ve sınırların saptanması için önerilen yöntemler ilk etap olarak, yapay veriler üzerinde test edilmiş ve tatmin edici sonuçlar elde edilmiştir. İkinci etap olarak, Adapazari havzasının gravite anomali haritası üzerinde uygulanmış ve olası çizgisellikler otomatik olarak elde edilmiştir. Ayrıca, yardımcı bilgi sağlamak amacı ile bölgedeki tortul

kalınlığı 3DINVER matlab programı kullanılarak hesaplanmıştır. Otomatik analiz sonuçları çalışma alanına ait jeolojik haritada gösterilen major ve minor faylarla kıyaslanmıştır. Sonuçlar, otomatik çizgisellik tanımlamanın görsel yorumdan daha fazla fay izi tanımladığını göstermişitir. Elde edilen çizgisellikler, jeolojik ve yardımcı bilgilerle birleştirilerek çalışma alanına ait tektonik oluşuma yeni bir yaklaşım getirilmeye çalışılmıştır.

Bu örnekler, major ve minör faylar olarak tanımlanan jeolojik özellikleri saptamada, Hough dönüşümü algoritmasının gravite anomali haritalarının kalitatif yorumunda kullanılabileceğini göstermiştir.

Anahtar Kelimeler: Hough Dönüşümü, Sınır analizi, Gravite, Çizgisellikler, Adapazarı Havzası, Türkiye.

INTRODUCTION

In the research on edge placing for geological sources, potential field data have key advantages. Speaking of the boundaries of geological bodies means speaking of the boundaries of geological resources and fault lines with different densities or magnetization. In the interpretation process for gravity and magnetic anomaly maps, geophysicists are usually interested in lineaments as an indicator of subsurface faults, contacts, and other tectonic features. In these anomaly maps, basic features used to explain fault-like structures include areas such as gradient zones and anomaly boundaries etc. Linear transformation areas and their parametric data play a key role in map interpretation.

Zones undergoing smooth linear transformation are easy to recognize visibly by experienced interpreters. However, such zones may not always be easily noticed in gravity and magnetic anomaly maps due to geological conditions. Such cases require approaches used to enhance lineaments. Directional derivative and discriminating anomalies are among the classical approaches used to overcome this problem. As the first step in revealing lineaments, image enhancement and edge detection procedures are performed on digitized input images. Edge detection and enhancement methods are employed to distinguish between geological bodies with different dimensions and depths. Discriminating methods are based upon zero break point or maximum positions by using vertical or horizontal derivatives, analytical signal amplitude or their various combinations. The theoretical basis for these methods is gravity anomalies of two-dimensional step model or reduced-to-pole magnetic anomaly characteristics. The maximum point of the first horizontal derivative or the zero breakpoint of the first and second vertical derivatives corresponds to the edges of the geological body boundaries. In geophysics, magnetic anomalies are used to detect the edge position for two- or one-dimensional vertical step model after they are transformed to pseudo-gravity anomalies or reduced-to-pole magnetic anomalies. Similar procedures apply to gravity anomalies as well. The edge enhancement methods commonly used in geophysics include vertical derivative, slope angle, θ map, and normalized standard change algorithms.

In addition to these methods, image processing techniques are frequently used in geology and geophysics to detect faults, large-scale ruptures, and other tectonic structures. Lineaments are often visually identified by experienced interpreters or can be obtained in the form of automatic or criteria-based lineament extraction techniques (Wiladis, 1999).

Image enhancement techniques are widely applied to geophysical images and make it easier to visually interpret them or to understand the geology. Most common enhancement techniques include contrast enhancement, edge detection, and filter types (Zhang et al., 2005). Some examples from the literature about edge detection are Blakely and Simpson (1986); McGrath (1991); Mallat and Zhong (1992); Moreau et al., (1997); Trompat et al., (2003). Approaches based on derivative calculations are the most classical methods used in geophysics. First horizontal and vertical derivatives, analytical signals, and grid filters are employed to enhance gravity and magnetic anomalies due to near-surface geological impacts (Zhang et al., 2005).

The upward continuation method is a process that involves separating long-wavelength anomalies from short-wavelength anomalies (Zhang et al., 2005). A gravity data processing technique CVUR (comparison of variance of upward-continuation residual) was proposed to remove the skin effects of surface layers and to estimate the deeper structure of the caldera (Komazawa, 1995). Tilt filter, which had been defined by Miller and Singh (1994), was successfully employed by Verduzco et al., (2004) to enhance weak and strong anomalies. Yunxuan

(1992) used continuation methods as well as the radon transform while removing unwanted lineaments from synthetic gravity anomaly maps. The radon transform was used by Pawlowski (1997) and Zhang et al., (2005-2006) to enhance potential field anomalies and to detect lineaments.

Some researchers have demonstrated that the Hough transform can be used to detect analytic and non-analytic curves. Initial research on the Hough transformation was confined to binary edge images. Later, in addition to straight lines, it was also used to detect other analytic shapes in 2D images such as the circle and ellipse. The main principle applied to detect this type of analytic shapes is the same as those applied in detecting straight lines and is based on an oriented structuring between the parameter definition in the Hough space and the edge points in image space. Later, the practice of drawing a point with a constant distance in the parameter plane was replaced by the generalized method of drawing points with varying distances depending on θ (degree) parameter on a line.

The present study employs the Hough transform and the methods developed by Blakely and Simpson (1986) in order to detect lineaments in gravity anomaly maps and to contribute to the tectonic formation in a part of the Adapazari basin. The first stage involves the automatic detection the lineaments and body boundaries in the region by applying the above methods on the gravity data. At the second stage, by taking geological information into account, an attempt is made to interpret the possible tectonic elements for the study area by combining the discontinuities belonging the same faults from among all detected. On the basis of the potential-field data, new covered faults are also identified in the region, in addition to those defined in previous studies.

METHODOLOGY AND NUMERICAL MODELS

Although there have been notable improvements in the procedures of quantitative modeling and inverse solution recently, qualitative geologic interpretation of gravity and magnetic data can also be performed manually or through image enhancement methods. Images derived from gravity and magnetic data using automatic image enhancement methods contribute to the mapping of tectonic elements. These maps show homogeneous zones with high or low density/susceptibility which are distinguished by discontinuity changes.

Large faults with substantial vertical displacement can be extracted from or located in the gradient zones in gravity and magnetic maps. Such faults are regional and termed as primary faults. This type of faults is easy to recognize in maps. However, what is important is to locate the faults which are masked by large mass anomalies and produce local gradient zones and it is quite difficult to identify such faults in anomaly maps. To reveal the anomalies of this type of faults, anomaly maps are subjected to enhancement procedures (Zeng et al., 1994). For qualitative and quantitative interpretation of anomalies of the fault model masked by regional areas, numerous image enhancement techniques applied to potential data have been developed. Image enhancement is a process whereby the quality of a digital image is improved.

Hough transform is method often used for automatic edge detection in model-based digital image processing. In model-based methods, pixels of an image do not mean anything on their own, but become meaningful only when they are considered as a whole together with the neighboring pixels. Hough transform is commonly based on the procedure of voting possible geometric shapes in an edge-detected image. Initially, it was a method first proposed by Hough (1962) to detect the lineaments in black and white images; however, it was later improved by Duda and Hart (1972) so as to identify different shapes in images. The transform allows representation of all sets of lines in the image plane on the two-parameter Hough plane (parameter plane) by the breakpoints of the sets of sinusoidal curves. In the method, sets of edge pixels in an image are detected after the pixel sets present on the same line on the image plane are mapped in the defined parameter plane in such a way that these pixels appear in the form of peaks in the parameter plane.

The Hough function transforms each non-zero point in an image (pixel) into a sinusoid in the parameter space (Fig. 1).

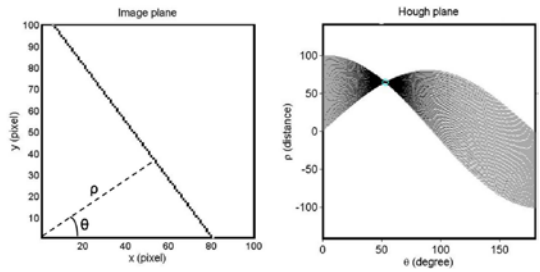

Figure 1. *Parameters of Hough transform in image plane (in the left), and Hough transform plane (in the right), (after Aydogan et al. 2013). ρ(pixel): distance of line in the image, θ(degree): orientation angle of the line from the origin.*

Şekil 1. Görüntü uzayında (solda) ve Hough transform uzayında (sağda) Hough transform parametreleri, (Aydogan ve diğ. 2013'den). ρ(piksel): görüntüdeki doğrunun uzaklığı, θ(derece): orijinden doğrunun yönelim açısı.

In the opposite case, each point in the parameter space corresponds to a straight line in the image. The classical transformation aims to identify the lines in an input image. The definition of a line in the parameter space was provided by Duda and Hart (1972) and was given as,

$$H(\rho,\theta) = \int_{-\infty}^{\infty}\int_{-\infty}^{\infty} f(x,y)\delta(\rho - xcos\theta - ysin\theta)dxdy. \quad (1)$$

The function *f(x,y)* in the relation is defined as the binary input image and δ is the impulse response function. The present study used the horizontal gradients of the input image to identify the lineaments in Hough space. Horizontal gradients of the input image *f(x,y)* in Eq. 1 are defined as follows;

$$F(x,y) = \frac{\partial f}{\partial x}\cos(\alpha) + \frac{\partial f}{\partial y}\sin(\alpha), \quad (\alpha\epsilon(0 - 360^0), \quad (2)$$

α in the expression denotes the direction of the maximum gradient. If the input image *f(x,y)* in the image space has the dimensions of mxn and if the points in the input image given in expression (1) are taken to have the directions of x and y and intervals of Δ*x* and Δ*y,* respectively, then the Hough space relationship based on the gradient function can be expressed as;

$$\mathrm{H}(\rho,\theta) = \sum_m \sum_n F(x,y)\delta(\rho - m\Delta xcos\theta - n\Delta ysin\theta). \quad (3)$$

The impulse response function contributes to the transformation of each point in the input image into a sinusoid in the parameter space using the following function:

$$\rho = m\Delta xcos\theta + n\Delta ysin\theta \quad (3)$$

Anomalies occurring in gradient zones are usually expressed in the form of potential field lineaments. Horizontal gradient maps are vivid, simple and intuitive derivate products that reveal the anomaly character and significant anomaly pattern discontinuities. These maps show the steepness of anomaly slope. Horizontal gradient maxima are formed over the steepest parts of potential field anomalies, while the minima appear over the flattest parts. Short-wavelength anomalies are simultaneously enhanced.

Lineament detection using Hough transform has been successfully applied in many fields. The method has the main advantage that it is relatively unaffected by the noise in images and the gaps in lines. The method is explained in detail in the following research; Wang et al., (1990), Carnieli et al., (1996), Capineri et al., (1998), Fitton and Cox (1998), Zhang et al., (2005; 2006), Cooper (2006), Aydogan (2008), Aydogan et al.(2013).

Figure 2 presents the block diagram of the algorithm. In order to visualize lineaments caused by the impacts of different masses, the method is applied on two digital models and a field dataset. The method's performance is compared to that of boundary value analysis algorithm as a classical method (Blakely and Simpson, 1986).

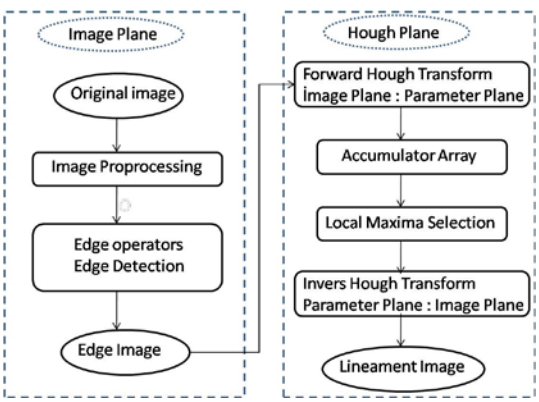

Figure 2. *Flowchart of procedures used in automatic lineament extraction by Hough transform (after Aydogan et al. 2013).*

Şekil 2. Hough dönüşümü ile otomatik çizgisellik çıkarımında kullanılan işlemlerin akış şeması (Aydogan ve diğ. 2013'den).

SYNTHETIC EXAMPLES

In this section, 2D test models are used to test the effectiveness of the Hough transform. In Figure 3a, a vertical finite prism is used for synthetic model 1 represented by Bouguer anomaly values. The prism had a length and width of 40 and 30 km, respectively; the depth of its upper and lower surfaces is 1 and 3 km, respectively; and its density difference is taken to be 0.1 g/cm^3. For the case when the proposed method is implemented, the accumulator matrix in the Hough space is shown in Fig. 3b, while Fig. 3c presents the obtained output image. The most significant advantage of the Hough transform is that it can generate an output image even on noisy images. Random noise is added to the model given in Figure 3a in an interval of -0.5 – 0.5 and the model and noisy anomaly values are shown in Fig. 4a. Fig. 4b shows the Hough space accumulator matrix, while Fig. 4c presents the output image. A close-to-real model is obtained even with noisy data. In order to test the method's reliability, the classical method of Blakely and Simpson (1986) is applied to the same model, the results of which are shown in Figs. 3d and 4d without and with noise, respectively. The method produces consistent results with those of Blakely and Simpson's method in the case of noiseless data, whereas the obtained results are closer to the real model with noisy data, which is also seen in Fig. 4c. The synthetic model 2 is also subjected to similar procedures and the results are shown in Figs. 5 and 6. For noisy anomaly generation, random values ranging between -0.5 and 0.5 are added. Model 2 consists of a finite prismatic mass. The length and width of prism A is 40 and 30 km, respectively; the depths of its upper and lower surfaces are 1 and 3 km, respectively; and the density difference is taken as 0.5 g/cm^3. On the other hand, we select the length and width of prism B as 40 and 20 km, respectively; the depth of its upper and lower surfaces as 1 and 3 km, respectively; and the density difference as 0.5 km. An examination of the results for this model demonstrates that the results of the method and of Blakely and Simpson are consistent in the case of noiseless data (Figs. 5c and 6c), but the method is more successful in the case of noisy data (Figs. 5d and 6d). As is clear from the results of both test models, the mass boundaries causing synthetic data could be successfully detected.

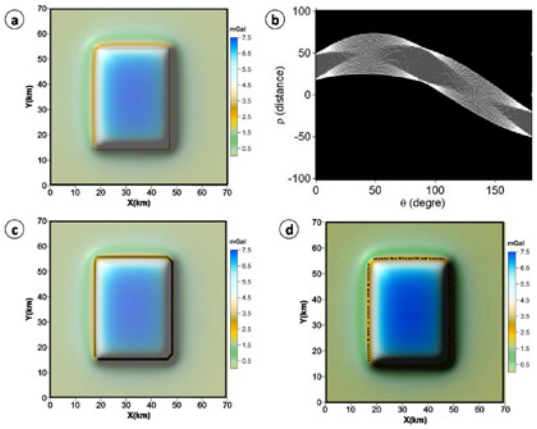

Figure 3. ***a)*** *The geometric position and gravity anomaly for theoretical model 1,* ***b)*** *Accumulator matrix,* ***c)*** *Source boundaries obtained by Hough algorithm,* ***d)*** *Source boundaries obtained by boundary analysis method (Blakely and Simpson, 1986).*

Şekil 3. a) Kuramsal model 1 için gravite anomalisi ve geometrik konumu, **b)** Akümülatör matrisi, **c)** Hough algoritması ile elde edilen kaynak sınırları, **d)** Sınır analiz yöntemi (Blakely and Simpson, 1986) ile elde edilen kaynak sınırları.

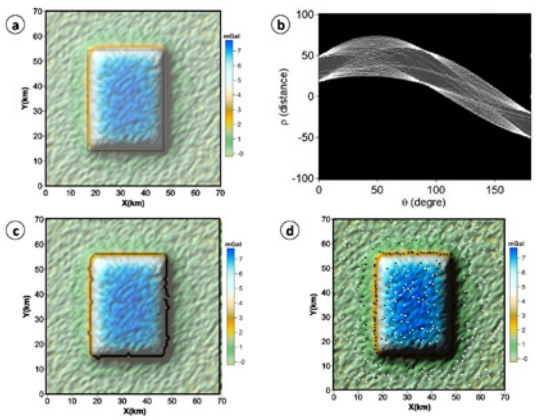

Figure 4. *Noisy anomaly,* ***a)*** *Geometric position and noisy gravity anomaly for theoretical model 1,* ***b)*** *Accumulator matrix,* ***c)*** *Source boundaries obtained by Hough algorithm,* ***d)*** *Source boundaries obtained by boundary analysis method (Blakely and Simpson, 1986).*

Şekil 4. Gürültülü anomali, **a)** Kuramsal model 1 için gürültülü gravite anomalisi ve geometrik konumu, **b)** Akümülatör matrisi, **c)** Hough algoritması ile elde edilen kaynak sınırları, **d)** Sınır analiz yöntemi (Blakely and Simpson, 1986) ile elde edilen kaynak sınırları.

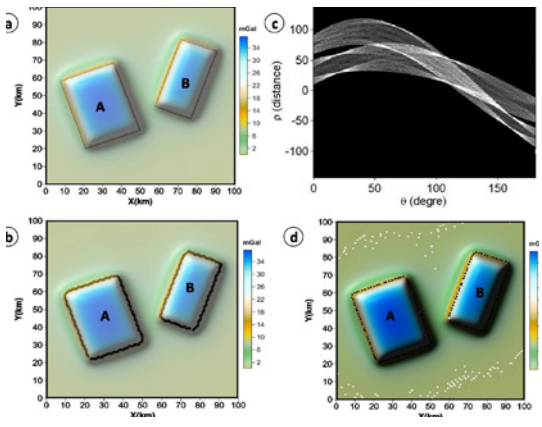

Figure 5. a) *Geometric position and gravity anomaly for theoretical model 2,* ***b)*** *Accumulator matrix,* ***c)*** *Source boundaries obtained by Hough algorithm,* ***d)*** *Source boundaries obtained by boundary analysis method (Blakely and Simpson, 1986).*

Şekil 5. a) Kuramsal model 2 için gravite anomalisi ve geometrik konumu, **b)** Akümülatör matrisi, **c)** Hough algoritması ile elde edilen kaynak sınırları, **d)** Sınır analiz yöntemi (Blakely and Simpson, 1986) ile elde edilen kaynak sınırları.

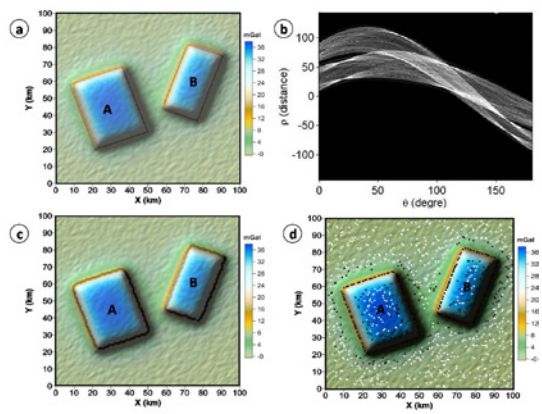

Figure 6. *Noisy anomaly,* ***a)*** *Geometric position and noisy gravity anomaly for theoretical model 2,* ***b)*** *Accumulator matrix,* ***c)*** *Source boundaries obtained by Hough algorithm,* ***d)*** *Source boundaries obtained by boundary analysis method (Blakely and Simpson, 1986).*

Şekil 6. Gürültülü anomaly, **a)** Kuramsal model 2 için gürültülü gravite anomalisi ve geometrik konumu, **b)** Akümülatör matrisi, **c)** Hough algoritması ile elde edilen kaynak sınırları, **d)** Sınır analiz yöntemi (Blakely and Simpson, 1986) ile elde edilen kaynak sınırları.

IMPLEMENTATIONS OF HOUGH TRANSFORM FOR REAL DATA

The topographic, geologic and gravity anomaly maps for the study area are taken from Komazawa et al.'s (2002) study analyzing the basic rock structure, Bouguer anomaly and microseismic SPAC and H/V analyses for the Adapazari basin. Figures 7 and 8 show the topographic and geologic maps of the region, respectively.

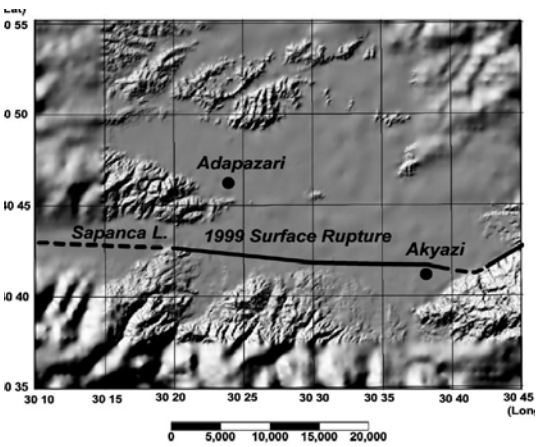

Figure 7. *Topographic map of Adapazari and surroundings (after Komazawa et al. 2002).*

Şekil 7. Adapazarı ve çevresine ait topoğrafya haritası (Komazawa ve diğ. 2002'den).

Adapazari, which is located in a basin of about 25x40 km^2, is a very flat alluvial plain. The hills on the northeastern foot of which is the downtown of Adapazari form a row which looks like a peninsula extending eastward into the basin. Sakarya River runs from south to north in the basin, and enters into Black Sea. The main North Anatolia fault of E–W strike forms the southern boundary, and the Duzce fault of NE–SW strike, the southeastern boundary. During the 1999 earthquake, surface ruptures with displacement up to 5 m appeared along the North Anatolia faults. There are steep mountain ranges of about 1000 m high on the south of the faults. The era of the basement rocks is different between the northern and southern parts: Devonian and Silurian in the northern part and Cretaceous in the southern part. Various rocks such as metamorphic, intrusive and volcanic rocks are observed along the faults. Volcanic ash–soil of Eocene covers these basement rocks.

Gravity Measurements were made out by Komazawa at al., (2002) in August 2000 and September

2001. A total of 645 data were taken using Lacoste and Romberg G-type, Scintrex SG-3M and ZLS-BURRIS.

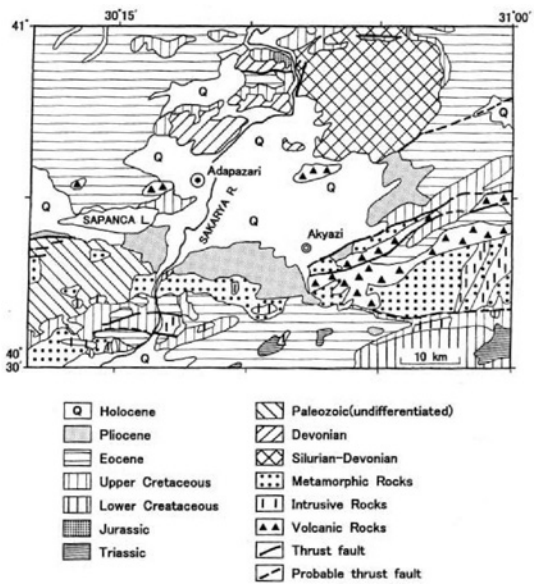

Figure 8. *Geologic map of Adapazari and surroundings (after Komazawa et al., 2002).*
Şekil 8. Adapazarı ve çevresine ait jeoloji haritası (Komazawa ve diğ. 2002'den).

Locations and altitudes of the sites were determined by the differential GPS technique with sufficient accuracy (within 1 m) for gravity analysis. The terrain correction was made with a digital map of 30 s mesh (GTOPO30) and digital local maps of 1/25.000. Figure 9 shows the Bouguer anomaly calculated using a reduction density of 2300 kg/m^3. The contour intervals are 1 mGal. They suggested that the anomaly has a typical feature of deep sedimentary basin surrounded by steep bedrock. There are two low-anomalies extending in E–W direction, suggesting at least two narrow depressions of bedrock in the basin. They said that it is very noticeable, dense distribution of linear contours extends in nearly E–W direction along about 40°48'N. The rate of change in gravity is comparable to those along the North Anatolia faults.

Horizontal gradient anomaly data obtained by implementing the gradient method on the Bouguer anomaly map to reveal the impacts on the sources with different depths are used as the input data in HT algorithm, and subsurface lineaments obtained at different levels are given in Fig. 10. Sediment thickness in the study area is obtained by using 3DINVER Matlab program (Ortiz and Agarwal, 2005) and Fig. 11 presents the map showing the sediment thickness. The sediment thicknesses are computed to range between -1.5 and .8 km in the region. Sediment thickness reaches its maximum (1.5 km) around Akyazi, where gravity anomaly values are about -35 mGal (Figure 9) and confirm the sediment thickness calculated. In Fig. 9, the region with the highest gravity value (35 mGal) is observed in the northern parts, and this is the region for which the lowest sediment thicknesses are calculated. A combined look at Figs. 9 and Figure 11 reveal the existence of an inverse relationship between sediment thicknesses and gravity values. In order to investigate the performance of HT algorithm, boundary detection algorithm is applied to the Bouguer anomaly map (Blakely and Simpson, 1986) and the body boundary map obtained is presented in Fig. 12.

By taking into account the maps in Figs. 7-12 and by combining the lineaments shown in Fig. 10, a map for possible fault traces is obtained and is given in Fig. 13. 28 lineaments are calculated as a result of the applied method and 13 fault traces are obtained after combining the related lineaments. In the lineament map (Fig. 10) the west-east oriented lineaments beginning in the north of Sapanca Lake and extending towards Akyazi (L1-L4) are combined and named as fault F1. This fault is consistent with the surface rupture of 1999 shown in Fig. 7 and forms the Northern Anatolia Fault (NAF) zone within the study area. This rupture is also congruous with the map obtained through boundary detection algorithm (Fig. 11). The L5-L7 lineaments starting in the north-west of Adapazari and extending towards the south-east are combined to form the F2 fault system. This fault appearing in the gradient zone in the gravity map is not observed in the geologic map. This fault trace is also supported by the boundary analysis map shown in Fig. 12. Fault F3 formed by combining the L8-L13 lineaments is located to north of Adapazari in an east-west direction. This fault is very evident in the gradient zone in the gravity anomaly map and also coincides with the region where there is a sharp drop in the sediment thickness map shown in Fig. 11. The fault that is roughly parallel to fault F1 is termed as the second major fault, which is partly seen in the boundary detection map shown in Fig. 12. The L14-L16 lineaments situated to north-east of the study area are named as fault F4, and are observed to be consistent with the fault in the geologic map.

The L17-L19 lineaments located to the south-west of the area form fault F5, which is partly confirmed by the boundary analysis map. We name lineament L20 as F6 and lineament L21 as F7 faults, which occurred in the gradient zones to the south-west of the area where gravity anomaly values are partly high. Lineament L22 forms a fault F8 and is seen to be consistent with the change in the gravity value. Lineaments L23 and L24 form the fault traces of F9 and F10, respectively, and are located to the north of the study area. Lineaments L25 and L26 in the south-east of Akyazi town are named as fault F11 and are supported by Fig. 12. Lineaments L27 and L28 are situated in the central parts of the study area and form faults F12 and F13, respectively. As is revealed by a combined examination of the maps in Figure 7-12, the fault traces obtained by the Hough algorithm are formed in the gradient zones in the Bouguer anomaly map (Fig. 13).

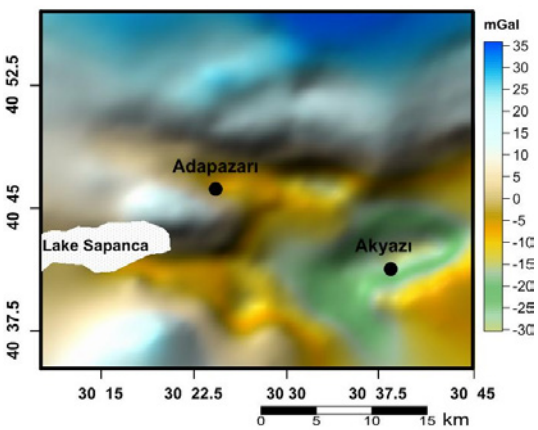

Figure 9. *Bouguer gravity anomaly map of Adapazari and surroundings obtained with reduction density of 2300 kg/m3. Contour interval is 1 mGal. Note the N–E trending low-anomalies in the northern part, and N–E and NE–SW trending low-anomalies in the southern part (after Komazawa et al., 2002).*

Şekil 9. 2300 kg/m^3 yoğunluk farkı ile elde edilen Adapazarı ve çevresine ait Bouguer anomali haritası. Kontur aralığı 1 mGal. K-D yönelimli yüksek anomaliler kuzey kesimde, ve K-D ve KD-GB yönelimli düşük anomaliler güney kesimde (Komazawa ve diğ. 2002'den).

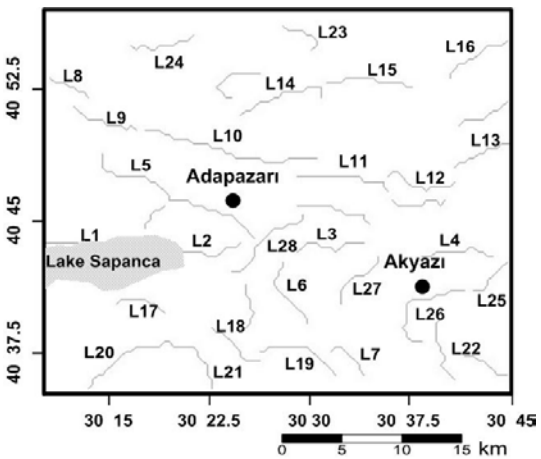

Figure 10. *Lineament map in Adapazari basin (Turkey) obtained from surface observations and Hough transform algorithm. Faults are explained in the text. The lineaments are superimposed on Bouguer anomaly map of Adapazari basin shown in Fig. 9 (Fig.13).*

Şekil 10. Yüzey ölçümleri ve Hough dönüşümü algoritmasından elde edilen Adapazarı havzasındaki çizgisellik haritası. Faylar makalede açıklanmıştır. Çizgisellikler Şekil 9'da gösterilen Adapazarı havzasına ait Bouguer anomali haritası üzerinde çizdirilmiştir (Şekil 13).

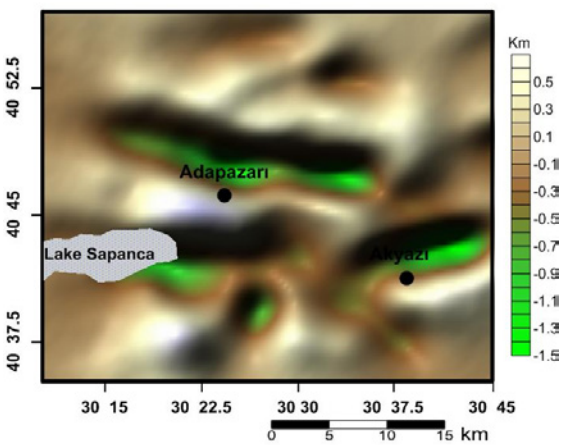

Figure 11. *3D basement relief of Adapazari basin obtained from application of 3DINVER matlab program (Ortiz and Agarwal, 2005) to gravity anomaly map of Fig. 9.*

Şekil 11. Şekil 9'da gösterilen gravite anomali haritası için 3DINVER matlab programı (Ortiz ve Agarwal, 2005) kullanılarak elde edilen Adapazarı havzasına ait 3B temel kabartma.

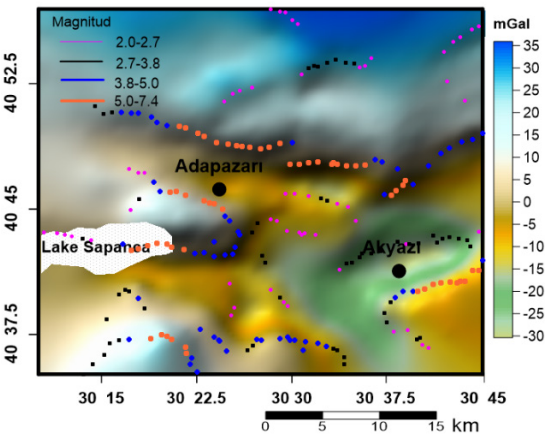

Figure 12. *Boundary map of Adapazari basin obtained from application of boundaries analysis algorithm (Blakely and Simpson, 1986).*

Şekil 12. Sınır analizi algoritması (Blakely and Simpson, 1986) ile elde edilen Adapazarı havzasının sınır haritası.

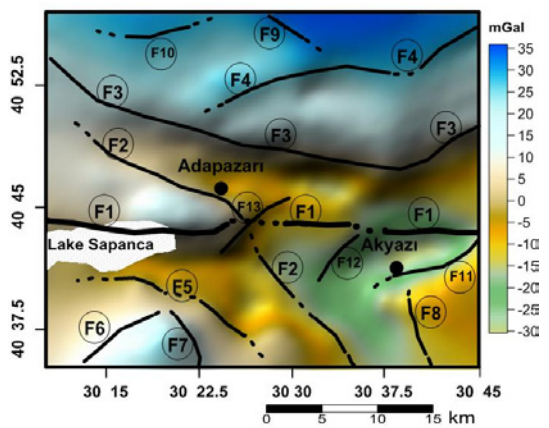

Figure 13. *Fault traces formed by combining the lineaments obtained by Hough algorithm in the Adapazari basin.*

Şekil 13. *Adapazarı havzasında Hough dönüşümü ile elde edilen çizgiselliklerin birleştirilmesi sonucu oluşturulan fay izleri.*

CONCLUSIONS

One of the purposes of structural interpretation for geophysical data is to map fault and rupture zones. These features can be characterized by marked lines and curves, and thus, can be identified within the process of lineament interpretation for processed potential-field data. Numerous algorithms have been developed to perform this procedure. It is quite difficult to predetermine which method would yield more meaningful results. The final selection of the processing and imaging procedure is based on experience as well as on which type and anomaly direction can assist enhancement.

Potential field signs for faults and ruptures require detailed information processing by using anomaly enhancement techniques. The present study investigated whether the Hough transform algorithm based on gradient calculations can be used to extract lineament information from the Bouguer anomaly map for the Adapazari basin and its vicinity. The method is implemented on field data after initially being tested on synthetic data. These examples allow for the qualitative and quantitative interpretation of gravity anomalies in order to identify the geologic features defined as major and minor faults. A comparison of the results obtained by the method implemented on the study area through a geologic map demonstrates that automatic lineament detection allows detecting more fault traces than a visual interpretation on a geologic map by geologists. Although the examples provided in the study mainly highlight the lineaments related to high-contrast boundaries, the proposed method can be used to detect both low- and high-contrast edges. Implementation of this method not only helps us directly identify the length and height of the lineaments throughout the edge detection process, but also contributes to the geologic analysis of lineaments.

ÖZET

Yer yüzüne yakın olmayan büyük kütlelerin neden olduğu rejyonal alanlarda düşey yada eğimli yer değiştirmelere sahip olan ve birincil faylar olarak isimlendirilen büyük faylar gravite ve manyetik anomali haritalardaki gradiyent zonlarında gözle görülebilir ve bu tip fayların görsel yorumlamaları yapılabilir. Jeofizikte en önemli sorunlardan biri büyük kütle anomalileri tarafından maskelenen ve yerel gradiyent zonlarını üreten ikincil fayların saptanması ve yorumlanması işlemidir. Bu tip fayların anomali haritalarında farkedilebilmeleri oldukça güç olup bunların anomalilerini ortaya çıkarmak ve yorumlamak amacı ile anomali haritalarına bir takım iyileştirme işlemleri uygulanmalıdır. Rejyonal alanlardaki kütleler tarafından maskelenen fay modellerine ait anomalilerin kalitatif ve kantitatif yorumu için potansiyel verilerine uygulanan pek çok görüntü iyileştirme tekniği geliştirilmiştir. Görüntü iyileştirme, sayısal bir görüntünün kalitesini artırma sürecidir. Hough dönüşüm algoritması model tabanlı

sayısal görüntü işlemede, çoğunlukla, otomatik kenar saptama amacı ile kullanılan bir iyileştirme yöntemidir. Model tabanlı yöntemlerde görüntüye ait pikseller kendi başlarına bir anlam ifade etmezken, etrafında bulunan piksellerle birlikte bir bütün olarak değerlendirildiklerinde bir anlam kazanmaktadırlar. Hough dönüşüm yöntemi, genel olarak, kenarları saptanmış bir görüntüdeki olası geometrik şekillerin oylanması esasına dayanmaktadır.

Bu çalışmada, gravite anomali haritalarına neden olan birincil ve ikincil fayların yerlerini saptamak ve Adapazarı havzasının bir bölümüne ait tektonik oluşuma katkı sağlamak amacı ile, görüntü işleme konularında sıklıkla kullanılan Hough dönüşümü algoritması önerilmiş ve uygulanabilirliği klasik yöntemlerle birlikte açıklanmaya çalışılmıştır. Önerilen yöntem ilk etap olarak, üretilen gürültülü/gürültüsüz gravite anomali verileri üzerinde test edilmiştir. Verilere neden olan yer altı kütle sınırları otomatik olarak saptanabilmiş olup elde edilen sonuçlar klasik yöntemlerden olan Blakely ve Simpson algoritması sonuçları ile göreceli olarak kıyaslanarak, genelde, büyük benzerlikler elde edilmiştir. İkinci adımda ise, arazi verisi olarak Adapazarı ve çevresine ait Bouguer anomali haritası üzerinde söz konusu algoritma uygulanıp jeolojik bilgiler de göz önünde tutularak, saptanan süreksizliklerden aynı faya ait olanların birleştirilmesi ile çalışma alanına ait olası tektonik yapı unsurları tümleşik bir çalışma sonucunda yorumlanmaya çalışılmıştır. Ayrıca, bu çalışmalara yardımcı olmak amacı ile yöreye ait bir tortul kalınlık haritası elde edilmiştir. Potansiyel alan verileri üzerinde, bölgede daha önce yapılan çalışmalar sonucunda tanımlanan fayların yanı sıra, üstü örtülü ve büyük kütleler tarafından maskelenen yeni ikincil faylar da saptanmıştır. Sonuç olarak, Hough dönüşümü algoritması jeofizik anomalilerine neden olan yer altı kütle dağılımlarının sınırlarının otomatik olarak saptanmasında ve görsel yorumunda kullanılabileceği kanısına varılmıştır.

ACKNOWLEDGEMENTS

This work is supported by the Department of Scientific Research Projects of İstanbul University with the number BYP/30317. The authors thank Prof. Dr. Rahmi Pınar(reviewer) and Assoc. Prof. Dr. M. Nuri Dolmaz(reviewer) for their reading and constructive comments on the manuscript. We appreciate very much their help.

REFERENCES

Aydogan, D., 2008, Extraction of lineaments from gravity anomaly maps by means of Hough transform: Application to Central Anatolia, e-Journal of New World Sciences Academy 3(4), 642-655.

Aydogan, D., Pinar, A., Elmas, A., Tarhan Bal, O. and Yuksel, S., 2013, Imaging of subsurface lineaments in southwestern part of the Thrace Basin from gravity data, Earth Planets Space, 65(4), 299-309.

Blakely, R. J., and Simpson, R. W., 1986, Approximating edges of source bodies from magnetic or gravity anomalies, Geophysics 51, 1494–1498.

Capineri, L., Grande, P., and Temple, J.A.G., 1998, Advances image processing technique for real time interpretation of Ground Penetrating Radar images, International Journal of Imaging Systems and Technology 9, (1), 51-59.

Carnieli, A., Meiseis, A., Fisher, L., and Arkin, Y., 1996, Automatic extraction and evaluation of geological linear features from digital remote sensing data using a Hough transform, Photogrammetric Engineering & Remote Sensing 62, (5), 525-531.

Cooper, G.R.J., 2006, Geophysical Applications of the Hough Transform, South African Journal of Geology 109, 555-560.

Duda, R. O., and Hart, P. E., 1972, Use of the Hough Transformation to Detect Lines and Curves in Pictures, Comm. ACM 15, 11-15.

Fitton, N.C., and Cox, S.J.D., 1998, Optimising the application of the Hough transform for automatic feature extraction from geoscientific images, Computers & Geosciences 24, (10), 933-951.

Hough, P. V. C., 1962, Method and Means for Recognizing Complex Patterns, US Patent, 3069654.

Komazawa, M., 1995, Gravimetric analysis of Aso Volcano and its interpretation, J. Geod. Soc. Japan 41, 17- 45.

Komazawa, M., Morikawa, H., Nakamura, K., Akamatsu, J., Nishimura, K., Sawada, S., Erken, A., and Onalp, A., 2002, Bedrock structure in Adapazari, Turkey—a possible cause of severe damage by the 1999 Kocaeli earthquake, Soil Dynamics and Earthquake Engineering 22, 829–836.

Mallat, S., and Zhong, S., 1992, Characterization of signals from multiscale edges, IEEE Trans-

actions on Pattern Recognition and Machine Intelligence 14, 710–732.

McGrath, P.H., 1991, Dip and depth extent of density boundaries using horizontal derivatives of upward-continued gravity data, Geophysics 56, 1533–1542.

Miller, H.G., and Singh, V., 1994, Potential field tilt- a new concept for location of potential field sources, Journal of Applied Geophysics 32, 213-217.

Moreau, F., Gibert, D., Holschneider, M., and Saracco, G., 1997, Wavelet analysis of potential fields, Inverse Problems 13, 165–78.

Ortiz, D.G., and Agarwal, B.N.P., 2005, 3DINVER.M: a MATLAB program to invert the gravity anomaly over a 3D horizontal density interface by Parker–Oldenburg's algorithm, Computers & Geosciences 31, 513–520.

Pawlowski, R.S., 1997, Use of slant stack for geologic or geophysical map lineament analysis, Geophysics 62, 1774–1778.

Trompat, H. Boschetti, F., and Hornby, P., 2003, Improved downward continuation of potential field data, Exploration Geophysics 34, (4), 249–256.

Verduzco, B., Fairhead,J.D., Green, C.M., and MacKenzie, C., 2004, New insights into magnetic derivatives for structural mapping, The Leading Edge 23, (2), 116-119.

Wang, J., and Howarth, P.J., 1990, Use of the Hough transform in automated lineament detection, IEEE Transactions on Geoscience and Remote Sensing 28, (4), 561-566.

Wiladis, D., 1999, Automatic lineament detection using digital elevation models with second derivative filters, Photogrammetric Engineering & Remote Sensing 65, (4), 453-458.

Yunxuan, Z., 1992, Application of the Radon transform to the processing of airborne geophysical data, Ph.D. thesis, Delft University of Technology.

Zeng, H. Zhang, Q., and Liu, J., 1994, Location of secondary faults from cross-correlation of the second vertical derivative of gravity anomalies, Geophysical Prospecting 42, 841-854.

Zhang, L.L., Hao, T., Wu, J., and Wang, J., 2005, Application of image enhancement techniques to potential field data, Applied Geophysics 2, (3), 145-152.

Zhang, L.L., Wu, J., Hao, T., and Wang, J., 2006, Automatic Lineament extraction from potential field images using the Radon transform and gradient calculation, Geophysics 71, (3), J31-J40.